# Global Correlation of Mesoscale Ocean Variability with Seafloor Roughness from Satellite Altimetry

Sarah T. Gille

Department of Earth System Science, University of California, Irvine

Mara M. Yale[1]

ERIM-International, Inc., Ann Arbor, Michigan

David T. Sandwell

Scripps Institution of Oceanography, University of California, San Diego

**Abstract.** Both seafloor bathymetry and eddy kinetic energy at the ocean surface can be estimated by making use of satellite altimeters. Comparing the two quantities shows that in regions of the ocean deeper than about 4800 m, surface eddy kinetic energy is greater over smooth abyssal plains than over rough bathymetry, while the opposite is true in shallower waters. Thus in the deep ocean, bottom roughness may dissipate eddy kinetic energy. A simple model indicates that the dissipation rate increases as root-mean-squared bottom roughness increases from 0 to 250 m and decreases to negative values (implying eddy generation) for higher roughness.

## Introduction

Seafloor roughness is important for a variety of oceanic processes. It is associated with intense vertical mixing [*Polzin et al.*, 1997] as well as with dissipation of both barotropic tidal energy [*Munk and Wunsch*, 1998] and barotropic mesoscale energy over the continental shelf [*Brink*, 1986]. Observations indicate that Lagrangian floats lose about half of their eddy kinetic energy when they move from smooth to rough bathymetry near 70°W south of the Gulf Stream [*Freeland et al.*, 1975]. Similarly, in atmospheric general circulation models, wave drag over rough topography is needed to remove momentum from wintertime westerly flows [*Palmer et al.*, 1986]. In this study we use satellite altimeter measurements to examine how seafloor roughness may help both to dissipate and to generate mesoscale eddy kinetic energy at the ocean surface.

Satellite altimeters use a downward-looking radar to measure the height of the sea surface relative to the known altitude of the satellite. The time-varying component of sea surface height is mostly due to eddy variability at the ocean surface, while the time-invariant component is dominated by

---

the Earth's gravity field, which at wavelengths < 200 km, is closely related to seafloor bathymetry. Our analysis makes use of both components.

## Eddy Kinetic Energy and Roughness

From the time-varying component of altimeter data, we estimated eddy kinetic energy ($E_K$) shown in Figure 1a. While many previous estimates of surface $E_K$ from altimetry have focused on measurements from a single satellite [*Sandwell and Zhang*, 1989; *Cheney et al.*, 1983; *Stammer*, 1997], our analysis merged TOPEX altimeter data [*Fu et al.*, 1994] from September 1992 through May 1997 with exact repeat European Remote Sensing Satellite (ERS-1 and ERS-2) data from May 1992 through November 1996. The ERS satellites pass over the same points every 35 days, providing denser spatial coverage than TOPEX achieves with its 10-day orbit. Due to design differences between the satellites, ERS orbits repeat less precisely than TOPEX orbits, potentially yielding a false measure of variability. Merging data from the two satellites increases spatial resolution and reduces errors in $E_K$.

We computed sea-surface slopes from along-track height measurements and processed the data following standard procedures to correct for tides and orbit errors [*Yale et al.*, 1995]. For TOPEX, ERS-1, and ERS-2, at each point along the groundtracks we removed the time-mean sea surface slope. Then we filtered residual sea surface slope profiles to retain wavelengths longer than 80 km, and computed the time variance. These results were converted to mean-squared velocities using the geostrophic relationship: $\langle v^2 \rangle = g^2 f^{-2} \langle (\partial \eta / \partial l)^2 \rangle$, where $v$ is the surface geostrophic velocity component normal to the local track orientation, $g$ is gravity, $f$ is the Coriolis parameter, and $\partial \eta / \partial l$ is the local along-track sea surface slope. Assuming that eddy variability is isotropic, we defined $E_K = \langle v^2 \rangle$ and computed the median variance of both ascending and descending tracks in 0.25° latitude by 0.2° longitude cells. Data were low-pass filtered to eliminate high-wavenumbers, where ERS and TOPEX differ, and then combined by computing local median $E_K$ and splining it onto a regular grid. The separate ERS and TOPEX variability estimates have a correlation co-
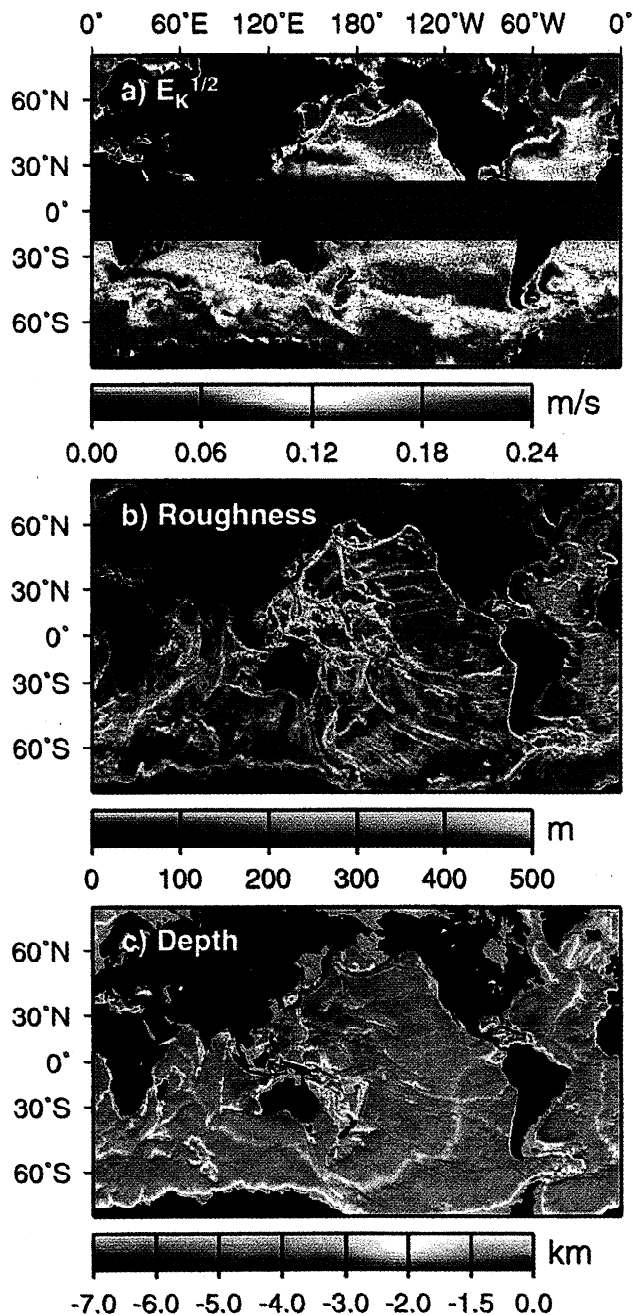
**Figure 1.** (a) Global ocean surface eddy kinetic energy, $E_K^{1/2}$, computed from altimeter data. (b) Global bottom roughness $r$. (c) Smoothed global bathymetry derived from ship soundings and altimeter-derived gravity anomalies [Smith and Sandwell, 1997].

efficient of 0.93, and the merged product is shown in Figure 1a. We estimate the measurement noise to be 0.03 to 0.04 m s$^{-1}$. Data equatorward of 20° are omitted because of the higher errors associated with small $f$.

Next we estimated seafloor roughness on a grid coregistered with the $E_K$ grid of Figure 1a. To do this, we high-pass filtered ($\lambda > 160$ km) global bathymetry that was derived from non-repeat orbit GEOSAT and ERS-1 altimeter measurements as well as available ship soundings [Yale et al., 1995; Smith and Sandwell, 1997]. This resulted in band-pass filtered topography since the altimeter-derived gravity does

not resolve features having wavelengths less than about $2\pi$ times the ocean depth ($\approx 20$ km). We squared the filtered bathymetry, applied a low-pass filter ($\lambda < 160$ km), and computed the square root to obtain roughness, $r$ [Smith, 1998]. The actual spatial variations in seafloor roughness are several times greater than shown in Figure 1b, because we have not resolved small-scale seafloor structures.

To first approximation, seafloor roughness is inversely related to the rate of seafloor spreading [Small and Sandwell, 1992; Smith, 1998] and also depends on sediment cover and seamount abundance. Because our roughness map is derived from the most complete seafloor topography dataset available, it includes the effects of sediment and newly discovered seamounts. Roughness is greatest near slow-spreading mid-ocean ridges such as the Mid-Atlantic Ridge and the Southwest Indian Ridge. For reference, Figure 1c shows smoothed ocean depth derived from ship soundings and altimeter-derived gravity anomalies [Smith and Sandwell, 1997].

## Low Roughness and High $E_K$

Close examination of the North Atlantic in Figure 1 suggests that regions of high $E_K$ (such as the core of the Gulf Stream) are located over smooth topography, while regions of rough topography near the Mid-Atlantic Ridge have low $E_K$. Similar patterns emerge near Campbell Plateau, southwest of New Zealand. Several factors may account for this anticorrelation between roughness and eddy kinetic energy.

Eddy activity could diminish over rough bathymetry, in part because regions of rough bathymetry tend to be shallower, and currents are steered around bathymetric obstructions, particularly at high latitudes [Sandwell and Zhang, 1989; Gille, 1994], so that $E_K$ due to baroclinic instability of currents will be stronger in deep water. To correct for the correlation between depth and roughness, in Figure 2a data were binned by local depth, and correlation coefficients were computed for seafloor roughness versus $\sqrt{E_K}$. For this analysis we consider only regions between 40° and 63°. Equatorward of 40° stratification and baroclinicity increase, decoupling surface eddy energy from bottom flow. Poleward of 63° TOPEX measures meridional velocities as it nears its 66° turning latitude and suffers uneven sampling due to seasonal sea ice. Our analysis excludes regions with $E_K < 0.005$ m$^2$ s$^{-2}$ in order to screen out low-energy areas where measurement noise may overwhelm the altimetric signal.

Figure 2b shows a histogram of ocean depth for the data points considered in Figure 2a. In the most common ocean depths, between about 3500 and 4500 m, the correlation coefficients between $\sqrt{E_K}$ and roughness are not distinguishable from zero. In regions shallower than 3000 m, $\sqrt{E_K}$ increases with roughness, suggesting that $\sqrt{E_K}$ may be generated as a response to rough topography. In regions deeper than 4800 m correlation coefficients are nearly always significantly negative, indicating that $\sqrt{E_K}$ and roughness are anticorrelated. In the latitude range we consider here, negative correlation coefficients at depths greater than 5200 m can be attributed to processes in the Argentine Basin; however when we considered a larger latitude range (not shown),
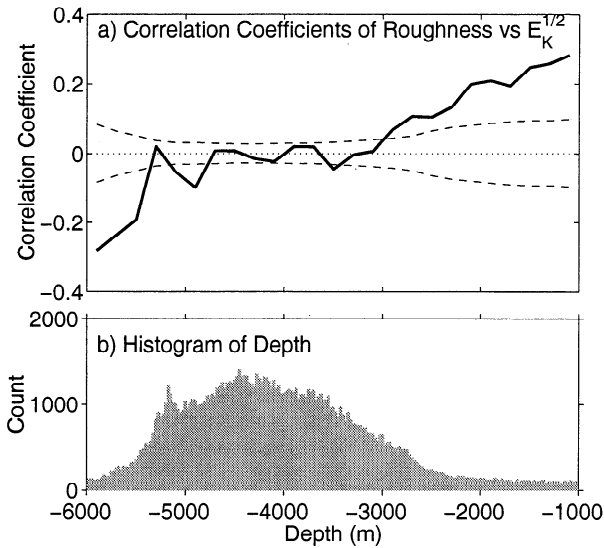
**Figure 2.** (a) Correlation coefficient of bottom roughness versus $E_K^{1/2}$ for data binned as a function of depth (solid line). The 95% confidence limits (dashed lines) indicate the range of correlation coefficients that are statistically indistinguishable from zero. (b) Histogram of ocean depths with same energy and latitude limits as above, sorted in 25 m bins.

we saw qualitatively similar negative correlations due to regions outside the Argentine Basin.

Based on Figure 2, we hypothesize that in the deep ocean roughness dissipates mesoscale energy either through a mechanism akin to "form stress" or by converting barotropic energy into baroclinic energy or internal gravity waves. We thus expect the effective bottom drag to be proportional to $r^2$ [*Brink*, 1986] or to $r$.

## An Advective Model for EKE Dissipation

Ocean models of energy generation and dissipation typically postulate a balance of the form:

$$\frac{dE_K}{dt} + \frac{E_K}{\tau} = F(t) \qquad (1)$$

where $F(t)$ is energy generation through wind forcing or baroclinic instability, and $\tau$ is a dissipation timescale [*Garrett*, 1991]. Estimates of $\tau$ range from 7 days for spin-up of the Antarctic Circumpolar Current [*Wearn and Baker*, 1980] to 81 days for tidal dissipation [*Munk*, 1997] to $O(1000)$ days for viscous spin-down [*Gill*, 1982].

Most eddy kinetic energy generation appears to result from the baroclinic instability of strong jet-like currents [*Stammer and Wunsch*, 1999]. Here we assume that $F(t)$ is zero outside of baroclinically unstable currents, and we hypothesize that $\tau$ depends on roughness. To test this, we examined the steady-state energy balance in the ocean's interior:

$$\frac{dE_K}{dt} = \mathbf{U} \cdot \nabla E_K = -\frac{E_K}{\tau}, \qquad (2)$$

where $\mathbf{U}$ is the large-scale, time-mean advective velocity. We estimated $\mathbf{U}$ by computing geostrophic surface velocities relative to 1000 m from Levitus climatology [*Levitus*,

1982], gridded at 1° resolution. The climatological data have been smoothed, and so the velocities are likely to indicate the direction and magnitude of flow but to underestimate local mean velocities. To calculate $dE_K/dt$, we computed discrete horizontal derivatives of $E_K$ at quarter-degree resolution, and we cubic splined the velocity fields onto the same locations as the $\nabla E_K$ estimates.

Figure 3 shows $-E_K^{-1} dE_K/dt = 1/\tau$ as a function of roughness. Results shown here represent data only from regions deeper than 4000 m, where anticorrelation or no correlation is expected. We used the same latitude and lower $E_K$ limits as in Figure 2 and also required that $E_K < 0.05$ m$^2$ s$^{-2}$ in order to screen out high-energy areas where baroclinic instability is likely to generate energy.

While individual points in Figure 3a indicate an enormous scatter, when we binned by bottom roughness and averaged, we found that $1/\tau$ is positive, indicating energy dissipation, and increases with $r$ for roughness values less than 250 m. Regions with $r$ between 100 and 250 m are responsible for about 10% more ocean dissipation compared with what we would predict if dissipation rates were constant everywhere. As roughness increases above 250 m, dissipation rate decreases to negative values implying net energy generation.

Although the qualitative variations in $\tau$ are robust, the exact values of $\tau$ depend partially on the definition used for $\mathbf{U}$ and on the ranges of latitude, $E_K$, and depth considered. The global trends are dominated by signals from the North Atlantic and the Southern Ocean which have rough topography generated by slow spreading mid-ocean ridges. In contrast, the seafloor of the North Pacific is smoother, and the statistics of this region deviate from the global results.
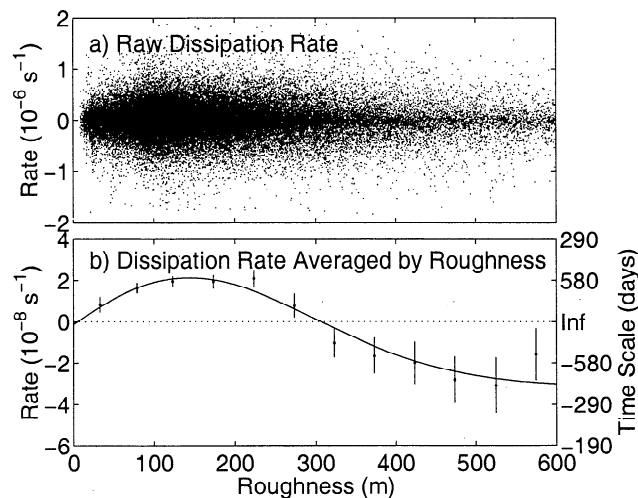


**Figure 3.** (a) Dissipation rate $-E_K^{-1} dE_K/dt = 1/\tau$ as a function of roughness for each data point. Positive $1/\tau$ indicates that $E_K$ is dissipated on length scales seen by satellite altimetry. The large scatter in dissipation rates shows that energy is both removed and added throughout the ocean. (b) Mean dissipation rate as a function of roughness (circles with error bars) and empirical fit (solid line). Data have been binned by roughness at 50 m increments. Error bars represent error of the mean and are equal to the standard deviation of all the data values, divided by the square root of the number of data points.

In this analysis, for $r$ between 0 and 250 m, dissipation rates correspond to $e$-folding time scales of 550 to 1450 days. These dissipation timescales are longer than barotropic tidal dissipation estimates, most likely because mesoscale variability is surface intensified and only indirectly controlled by bathymetry. Observed dissipation timescales are also longer than scales imposed in current numerical ocean models [*Semtner and Chervin*, 1992; *Maltrud et al.*, 1998]; biharmonic viscosities of order $10^{19}$ cm$^4$ s$^{-1}$ correspond to time scales of $(L/2\pi)^4/\nu = 10$ to 170 days for ocean variability with wavelengths from 100 to 200 km. The long decay timescales indicated by our observations, particularly over smooth bathymetry, may not be readily accessible with current numerical models due to numerical stability constraints.

We fit observed values of $1/\tau$ to the function $\beta(r - r_0)\exp(-r^2/\alpha^2) + \gamma$. Our best estimated fit, plotted as a solid line in Figure 3b, had parameters $\alpha = 270 \pm 30$, $\beta = 2.8 \times 10^{-10} \pm 0.5 \times 10^{-10}$, $r_0 = -110 \pm 60$, $\gamma = -3.1 \times 10^{-8} \pm 0.9 \times 10^{-8}$, where error bars were estimated using a Monte Carlo process. This function captures both the linear increase in $1/\tau$ at small $r$ and the fall in $1/\tau$ with increasing $r$.

The deep ocean dependence of dissipation on roughness shown here is statistically different from zero on a global scale. However, this simple model does not attempt to capture anything other than a balance between energy generation in strong currents and dissipation in the ocean interior. Mid-ocean baroclinic instability, coastal processes, wind forcing, and buoyancy forcing may also influence $E_K$. Thus there is no reason to expect any given region of the ocean to conform to the global trend, and not surprisingly, as Figure 3a indicates, individual dissipation estimates may scatter substantially about their global means.

## Summary

Our findings indicate that the character of bottom topography partially determines how much of the mesoscale energy that is generated through baroclinic instability is dissipated at any given location in the ocean. In the deep ocean, smooth topography dissipates less energy than rough topography, while extremely rough or shallow topography may be sufficiently large to generate eddies. Ultimately the influence of topographic roughness on eddy processes is important, not only for identifying where mixing occurs in the ocean, but also for parameterizing mixing rates in climate models, and for understanding how past seafloor morphology might have led to different mixing patterns than we see today.

## References

Brink, K., Topographic drag due to barotropic flow over the continental shelf and slope, *J. Phys. Oceanogr.*, *16*, 2150–2158, 1986.

Cheney, R. E., J. G. Marsh, and B. Beckley, Global mesoscale variability from collinear tracks of SEASAT altimeter data, *J. Geophys. Res.*, *88*, 4343–4354, 1983.

Freeland, H. J., P. B. Rhines, and T. Rossby, Statistical observations of the trajectories of neutrally buoyant floats in the North Atlantic, *J. Mar. Res.*, *33*, 383–404, 1975.

Fu, L. L., E. J. Christensen, Yamarone, C. A., Jr., M. Lefebvre, Y. Ménard, M. Dorrer, and P. Escudier, TOPEX/POSEIDON mission overview, *J. Geophys. Res.*, *99*, 24,369–24,381, 1994.

Garrett, C., Paradigm lost, *Proceedings, Hawaii Winter Workshop*, pp. 433–449, 1991.

Gill, A. E., *Atmosphere-Ocean Dynamics*. Academic Press, New York, 1982.

Gille, S. T., Mean sea surface height of the Antarctic Circumpolar Current from Geosat data: Method and application, *J. Geophys. Res.*, *99*, 18,255–18,273, 1994.

Levitus, S., Climatological atlas of the world oceans, Tech. rep., NOAA, U.S. Govt. Print. Off., Washington, DC, Prof. Paper 13, 1982.

Maltrud, M. E., R. D. Smith, A. J. Semtner, and R. C. Malone, Global eddy-resolving ocean simulations driven by 1985-1994 atmospheric winds, *J. Geophys. Res.*, *103*, 30,825–30,853, 1998.

Munk, W., Once again: once again—tidal friction, *Prog. Oceanog.*, *40*, 7–35, 1997.

Munk, W., and C. Wunsch, Abyssal recipes II: energetics of tidal and wind mixing, *Deep Sea Res. I*, *45*, 1977–2010, 1998.

Palmer, T. N., G. J. Shutts, and R. Swinbank, Alleviation of a systematic westerly bias in general circulation and numerical weather prediction models through an orographic gravity wave drag parametrization, *Quart. J. R. Met. Soc.*, *112*, 1001–1039, 1986.

Polzin, K. L., J. M. Toole, J. R. Ledwell, and R. W. Schmitt, Spatial variability of turbulent mixing in the abyssal ocean, *Science*, *276*, 93–96, 1997.

Sandwell, D. T., and B. Zhang, Global mesoscale varability from Geosat Exact Repeat Mission: Correlation with ocean depth, *J. Geophys. Res.*, *94*, 17,971–17,984, 1989.

Semtner, A. J., and R. M. Chervin, Ocean general circulation from a global eddy-resolving model, *J. Geophys. Res.*, *97*, 5493–5550, 1992.

Small, C., and D. T. Sandwell, An analysis of ridge axis gravity roughness and spreading rate, *J. Geophys. Res.*, *97*, 3235–3245, 1992.

Smith, W. H. F., and D. T. Sandwell, Global seafloor topography from satellite altimetery and ship depth soundings, *Science*, *277*, 1956–1962, 1997.

Smith, W. H. F., Seafloor tectonic fabric from satellite altimetry, *Ann. Rev. Earth Plan. Sci.*, *26*, 697-747, 1998.

Stammer, D., Global characteristics of ocean variability estimated from regional TOPEX/POSEIDON altimeter measurements, *J. Phys. Oceanog.*, *27*, 1743–1769, 1997.

Stammer, D., and C. Wunsch, Temporal changes in eddy energy of the oceans, *Deep Sea Res. II*, *46*, 77–108, 1999.

Wearn, Jr., R. B., and D. J. Baker, Jr., Bottom pressure measurements across the Antarctic Circumpolar Current and their relation to the wind, *Deep Sea Res.*, *27A*, 875–888, 1980.

Yale, M. M., D. T. Sandwell, and W. H. F. Smith, Comparison of along-track resolution of stacked Geosat, ERS 1 and TOPEX satellite altimeters, *J. Geophys. Res.*, *100*, 15,117–15,127, 1995.

S. T. Gille, Department of Earth System Science, University of California, Irvine, CA 92697-3100. (e-mail: sgille@uci.edu)

M. M. Yale, The Mathworks, Inc., 3 Apple Hill Drive, Natick, MA 01760-2098. (e-mail: myale@mathworks.com)

D. T. Sandwell, Scripps Institution of Oceanography, UCSD, La Jolla, CA 92093-0225. (e-mail: dsandwell@ucsd.edu)